The Meteoritical Society

Meteoritics & Planetary Science 44, Nr 11, 1695–1706 (2009)
Abstract available online at http://meteoritics.org

Rietveld analysis of X-ray powder diffraction patterns as a potential tool for the identification of impact-deformed carbonate rocks

Sarah A. HUSON*, Franklin F. FOIT, A. John WATKINSON, and Michael C. POPE

School of Earth and Environmental Sciences, Washington State University, Pullman, Washington 99164, USA
*Corresponding author. E-mail: sahuson@hotmail.com

(Received 20 March 2008; revision accepted 15 August 2009)

Abstract–Previous X-ray powder diffraction (XRD) studies revealed that shock deformed carbonates and quartz have broader XRD patterns than those of unshocked samples. Entire XRD patterns, single peak profiles and Rietveld refined parameters of carbonate samples from the Sierra Madera impact crater, west Texas, unshocked equivalent samples from 95 miles north of the crater and the Mission Canyon Formation of southwest Montana and western Wyoming were used to evaluate the use of X-ray powder diffraction as a potential tool for distinguishing impact deformed rocks from unshocked and tectonically deformed rocks. At Sierra Madera dolostone and limestone samples were collected from the crater rim (lower shock intensity) and the central uplift (higher shock intensity). Unshocked equivalent dolostone samples were collected from well cores drilled outside of the impact crater. Carbonate rocks of the Mission Canyon Formation were sampled along a transect across the tectonic front of the Sevier and Laramide orogenic belts.

Whereas calcite subjected to significant shock intensities at the Sierra Madera impact crater can be differentiated from tectonically deformed calcite from the Mission Canyon Formation using Rietveld refined peak profiles, weakly shocked calcite from the crater rim appears to be indistinguishable from the tectonically deformed calcite. In contrast, Rietveld analysis readily distinguishes shocked Sierra Madera dolomite from unshocked equivalent dolostone samples from outside the crater and tectonically deformed Mission Canyon Formation dolomite.

INTRODUCTION

The physical record of impact structures on the surface of the Earth dates from 3.5 Ga (Grieve 1998) and it is thought that impact cratering was an essential process even earlier in Earth's history (Ryder 2002). Putative impact structures commonly are identified by the presence of meteorite fragments, siderophile element anomalies, and specific shock deformational features including shatter cones, planar deformation features (PDFs) in minerals, diaplectic glass, and melting features (French 1998). Circular or nearly circular geomorphic structures lacking these distinctive features of suspected impact origin often are the subject of controversy (e.g., the Silverpit structure; Stewart and Allen 2002; Underhill 2004; Reimold 2007).

Currently, there are 176 impact structures confirmed in the Earth Impact Database (www.unb.ca/passc/ImpactDatabase). Criteria used to confirm circular structures on the Earth's surface as meteorite craters vary with target rock type, age, bolide size, and amount of material removed by erosion. However, exposure to short-lived shock pressure is a unique characteristic of the target rocks at all impact structures. Therefore, a method of identifying minerals/rocks subjected to shock metamorphism, but lacking the usual shock deformational features, would be extremely useful for distinguishing suspected impact structures from non-impact generated structures. Past studies, X-ray diffraction (XRD) and petrographic, often focused on both experimentally and naturally shocked silicate minerals due to the abundance and robust nature of these minerals at the Earth's surface (Hörz 1968; Short 1968; Hörz and Quaide 1973; Grieve et al. 1996). An X-ray powder diffraction method for evaluating shock deformation levels within impact craters formed in carbonate host rocks was developed by Skála and Jakeš (1999). A broadening (i.e., increase in peak width) and reduction in intensity of CuKα X-ray diffraction peaks in the 2θ° range 56–62° was observed in impact-shocked carbonate from the Kara crater (~65 km diameter) in Russia and the Steinheim Basin (3.8 km diameter) in Germany when compared to diffraction peaks of unshocked standards (Skála and Jakeš 1999). Furthermore, peak broadening and loss of peak intensity increased with increasing shock pressure (Skála and Jakeš 1999). However, XRD peak broadening in carbonate samples

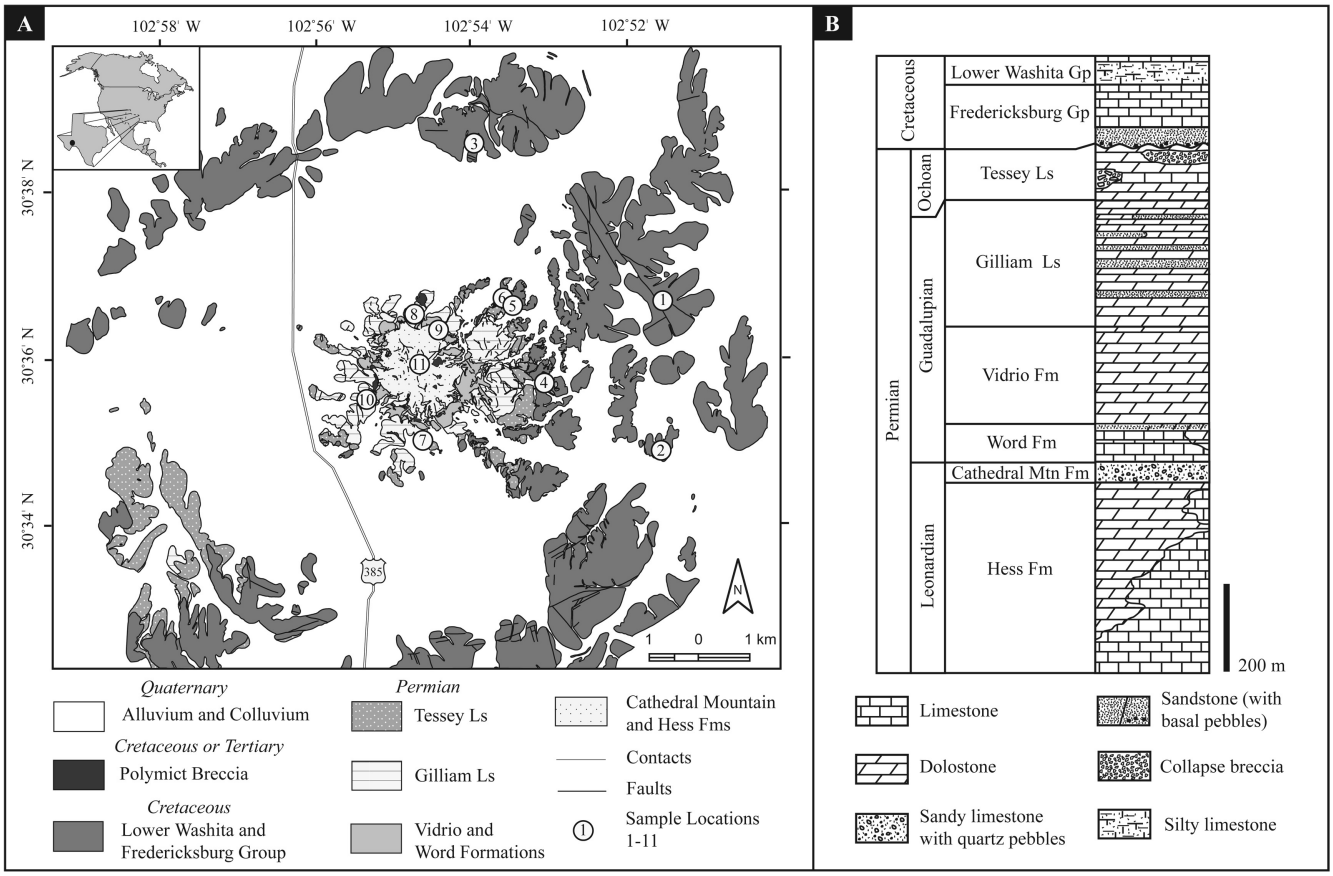

Fig. 1. a) Geologic map of Sierra Madera (modified from Wilshire et al. 1972). 1 = Kwf 1, 2 = Kwf 2, 3 = Kwf 3, 4 = Kwf 4, 5 = Kwf 5, 6 = Pt, 7 = Pg B1, 8 = Mlb, 9 = Pw, 10 = Pv, 11 = Ph. b) Stratigraphic column for rocks exposed at Sierra Madera.

from Meteor Crater (1.2 km diameter), Arizona, and nearby Canyon Diablo did not show the expected relationship of increased peak broadening with increasing shock effects from structure rim to structure center. These results were attributed to a non-uniform distribution of shock pressure during the impact event (Burt and Pope 2001; Burt et al. 2005). In an effort to resolve this discrepancy, carbonate and siliciclastic samples from the Sierra Madera impact structure (12 km diameter) in Texas were analyzed using XRD techniques adopted from Skála and Jakeš (1999). Preliminary studies of the Sierra Madera carbonates indicated increased peak broadening in shatter cone samples (Huson et al. 2006a, 2006b).

In the present study, XRD patterns of calcite and dolomite from the Sierra Madera impact structure are compared to those of unshocked equivalent carbonate samples from outside the structure, unshocked carbonate samples from the Mississippian Mission Canyon Formation of the northern Rocky Mountains, United States, and to unshocked/undeformed mineral standards. The objective is to determine whether XRD patterns of the shocked carbonates can be distinguished from XRD patterns of carbonates that were deformed solely by terrestrial processes (e.g., burial or tectonism). This study has implications for using XRD pattern analysis as a tool for the identification of effects of shock metamorphic processes where conventional impact characteristics (i.e., shatter cones and PDFs in minerals) are lacking or poorly developed, especially as ~30% of all terrestrial impact structures formed primarily in carbonate rocks (Grieve and Robertson 1979).

GEOLOGIC SETTINGS

Sierra Madera Impact Structure

The Sierra Madera impact structure, located near Fort Stockton, Texas, is a well-exposed, eroded remnant of a complex, 12 km diameter impact structure (Eggleton and Shoemaker 1961; Wilshire and Howard 1968; Howard et al. 1972; Wilshire et al. 1972). The central uplift is composed of steeply dipping, folded, and faulted Upper Permian strata (Fig. 1). Lower Cretaceous rocks occur along the eastern margin of the central uplift. The Permian Hess Formation, the oldest stratigraphic unit exposed in the central uplift, was displaced vertically at least 790 m during the excavation and modification stage of structure development (Wilshire et al. 1972). The crater rim at Sierra Madera is composed of eroded Lower Cretaceous carbonate and siliciclastic rocks with

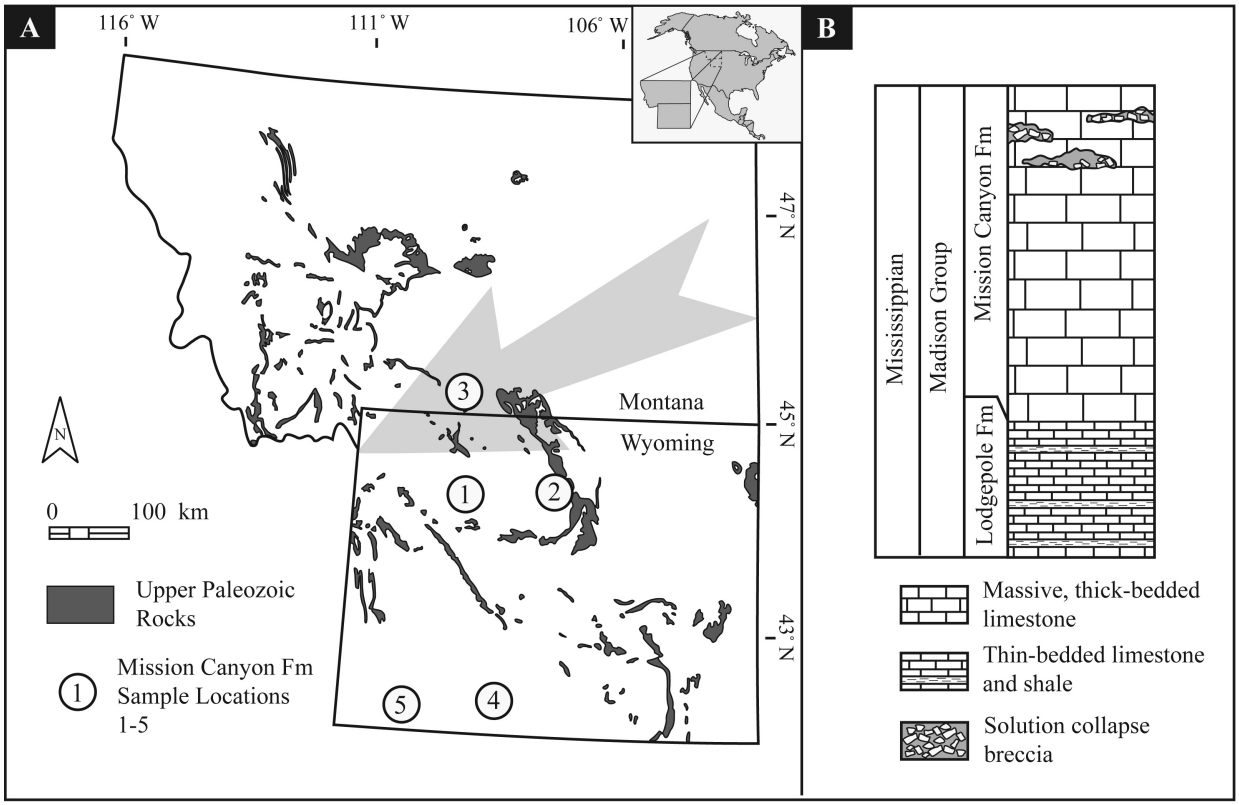

Fig. 2. a) Location of Mission Canyon Formation samples. 1 = Shoshone Canyon (SH), 2 = Sheep Mtn (SM), 3 = Benbow Mine (BM), 4 = UPR, 5 = Church Buttes (CB). Gray arrow indicates increasing burial depth and deformation. b) General stratigraphic column of the Mission Canyon Formation.

exception of the southwest side where stream incision has exposed Upper Permian strata. Rim strata are exposed ~30–60 m above the alluvium-filled ring depression and generally dip 0–5° radially, though at some locations the dip can be as great as 30°. The Upper Permian units at Sierra Madera were deposited on the southeast side of the Delaware Basin, a major depositional basin during the late Permian. The strata record a gradual in-filling and restriction of the basin. Lower Cretaceous rocks were deposited in a fluvial/deltaic to shallow water marine setting (Hill 1996). Post-impact erosion has removed an estimated 600 m of material from the crater rim (Wilshire et al. 1972). Past studies at Sierra Madera documented shock deformation features including shatter cones in siltstone and fine-grained sandstone, PDFs in quartz, grain fracturing, impact-induced brecciation, and deformed carbonate minerals (Dietz 1960; Eggleton and Shoemaker 1961; Howard and Offield 1968; Wilshire et al. 1972; Huson et al. 2005).

Unshocked Equivalent Dolostone Samples

Ninety-five miles north of the Sierra Madera impact structure, the equivalent Queen and Yates Formations were deposited on the northern edge of the Delaware Basin during the late Permian. These formations were deposited in a shallow shelf and later evaporitic environment as the Delaware Basin gradually became restricted (Hill 1996).

Mission Canyon Formation

The Lower Mississippian (Late Osagean-Middle Meramecian) Mission Canyon Formation in western Wyoming and southwestern Montana records shallow water carbonate deposition along a broad carbonate shelf that deepened westward during the Antler Orogeny (Late Devonian to Early Mississippian; Fig. 2; Sando 1976; Smith and Dorobek 1993). This unit was subsequently altered by Late Mississippian karstification and dolomitization and documents deep to shallow burial from west to east (Sando 1988; Smith and Dorobek 1993). Additional deformation of Paleozoic-Mesozoic strata of southwestern Montana and western Wyoming occurred during the Cretaceous-Paleogene Sevier and Laramide orogenies (Snoke 1993).

EXPERIMENTAL

Sample Collection and Preparation

Fine-grained dolostone and limestone samples were collected from the central uplift and eroded crater rim of the

Table 1. X-ray powder diffraction samples.

Sample	Composition	Sedimentary characteristics	Deformational features[1]	Lithology[2]
Sierra Madera samples				
Crater rim				
Kwf 1	Calcite	Fossils, fine-grained matrix	–	WS
Kwf 2	Calcite	Rare fossil fragments, fine-grained	–	MS
Kwf 3	Calcite	Fine-grained	F	MS
Central uplift				
Kwf 4	Calcite	Fine-grained	–	MS
Kwf 5	Calcite	Fossil fragments, fine-grained matrix	–	WS
Pt	Dolomite	Matrix supported breccia	B	Mono
Pg	Dolomite	Fine-grained	F, SC	MS
Mlb	Dolomite	Matrix supported breccia	B	Mono
Pv	Dolomite	Fine-grained	SC	MS
Pw	Dolomite	Fossils, fine-grained matrix	–	WS-PS
Ph	Dolomite	Fine-grained	SC	MS
Unshocked equivalent samples				
Queen/word	Dolomite	Fine-grained	–	MS
Yates/gilliam	Dolomite	Fine-grained	–	MS
Mission Canyon samples				
Shoshone Canyon				
SH 1	Calcite	Fine-grained	–	MS
SH 2	Dolomite	Recrystallized	Fc	DS
Sheep Mountain				
SM 1	Calcite	Fine-grained	–	MS
SM 2	Dolomite	Fine-grained	–	DS
Benbow Mine				
BM 1	Calcite	Fine-grained	–	MS
BM 2	Dolomite	Fine-grained	–	DS
UPR				
UPR[3]	Dolomite	Fine-grained	Fc	DS
Church Buttes				
CB 1	Calcite	Medium-fine grained	–	MS
CB 2	Dolomite	Fine-grained	–	DS
CB 3	Dolomite	Fine-grained	–	DS

[1]F = fractures; Fc = fractures filled with coarse calcite; B = brecciation; SC = shatter cones.
[2]MS = mudstone; WS = wackestone; WS-PS = wackestone-packstone; Mono = monomict impact generated breccia; DS = dolostone; LS = limestone.
[3]Contains visible sulfur.

Sierra Madera impact structure (Fig. 1; Table 1). Unshocked samples of the dolomitic Queen and Yates Formations, equivalent to the Upper Word and Gilliam Limestone at Sierra Madera, were collected from the Austin Core Facility in Austin, Texas. The cores were located in the North Ward-Estes Oil Field in Ward County, Texas, 95 miles north of the Sierra Madera impact structure. The authors were not able to obtain unshocked calcite-rich samples from outside the crater structure.

Fine-grained samples of dolostone and limestone were collected also from the Mission Canyon Formation of the Madison Limestone Group of southwest Montana and western Wyoming (Fig. 2; Table 1). Three optically clear samples of quartz, Iceland spar, and dolomite from Washington State University's School of Earth and Environmental Sciences (WSU SEES) mineral collection served as unshocked standards for comparison. All samples were ground under isopropyl alcohol using a mortar and pestle and the powders were passed through a 27 μm mesh sieve.

Sample Compositional Characterization

Since compositional differences can lead to XRD peak position and breadth variability (Fiquet et al. 1994), the magnesium, iron, and calcium content of all calcite and dolomite samples were analyzed using a Cameca electron microprobe and a JEOL 8500 F Field Emission electron microprobe in the WSU SEES GeoAnalytical Laboratory. No other elements were observed in more than trace amounts.

Table 2. Electron microprobe analytical data.

	Oxide wt%				
Sample name	MgO	FeO	CaO	CO_2[1]	Total oxide wt%
CALSTD	0.00	0.02	56.88	43.76	100.66
Sierra Madera samples					
Kwf 1	0.27	0.02	55.81	43.98	100.08
Kwf 2	0.40	0.06	54.60	44.25	99.30
Kwf 3	0.39	0.00	55.89	43.96	100.24
Kwf 4	0.50	0.01	55.49	44.03	100.03
Kwf 5	0.56	0.09	53.66	44.46	98.76
Mission Canyon samples					
SH 1	0.39	0.01	56.97	43.76	101.14
BM 1	0.30	0.00	55.86	43.98	100.14
CB 1	0.20	0.01	53.84	44.53	98.57
SM 1	0.30	0.01	55.08	44.18	99.56
DOLSTD	21.72	0.08	30.61	47.67	100.08
Sierra Madera samples					
Ph	20.60	0.01	31.72	47.55	99.88
Mlb	20.22	0.03	32.02	47.51	99.79
Pw	20.58	0.04	29.94	48.02	98.58
Pv	20.64	0.06	30.28	47.92	98.90
Pg	21.43	0.39	30.45	47.51	99.91
Pt	21.35	0.87	30.40	47.51	100.13
Mission Canyon samples					
SM 2	20.95	0.05	31.48	47.55	100.04
BM 2	21.24	0.01	31.22	47.60	100.07
CB 2	21.22	0.02	31.27	47.58	100.09
CB 3	21.31	0.02	31.22	47.58	100.14
SH 2	21.02	0.07	31.24	47.60	99.93
UP 1	21.51	0.02	31.03	47.61	100.16
Unshocked equivalent samples					
Yates	21.47	0.31	29.72	NA	99.38
Queen	21.36	0.37	30.14	NA	99.64

[1]Calculated from stoichiometry.

Polished grain mounts of the coarser size (45–63 μm) fraction of each sample used for XRD analysis were carbon coated and analyzed; sample compositions are presented in Table 2. The experimental parameters were: 15 kV acceleration voltage, 15 nA beam current, 4 μ beam diameter and 10 s dwell time on peak and background. The calibration standards (analytical line and spectrometer crystal) were: calcite (CaKα, PET), Obendorf dolomite (MgKα, TAP), and Irugtut siderite (FeKα, LiF).

All samples used in this study were also examined petrographically to determine whether there were noticeable compositional differences between sample sets that may lead to preferential grouping. In calcite-rich samples, both Sierra Madera and Mission Canyon Formation samples contain micritic limestone with bioclasts, peloids, and intraclasts. Abundances of allochems vary within each sample. Dolomite-rich samples have less variability, with both Sierra Madera and Mission Canyon Formation samples containing fine-grained dolomite and no allochems. The unshocked Queen and Yates Formation samples contain fine-grained dolomite with allochems. There is no indication of an enrichment of allochems or changes in grain size for either calcite-rich or dolomite-rich samples that would group samples preferentially.

X-Ray Powder Diffraction Analysis

XRD patterns were collected using CuKα radiation and a Siemens Kristalloflex Diffractometer equipped with a graphite diffracted beam monochromator and a scintillation detector. A combination of beam divergence and receiving slits yielding an instrument profile breadth of 0.083° 2θ for the 311 reflection of silicon powder were used (Foit 1992). The <27 μm powders were sifted onto a vaseline-coated, quartz zero background plate to reduce preferred orientation of the grains (Foit 1992). The diffractometer was operated at 35 kV and 30 mA and the samples were step-scanned over the range 15°–120° 2θ using a 0.02° 2θ step and dwell time of 10 sec. Although the samples

were scanned from 15°–120° 2θ, only the portion of the scan covering 55–69° 2θ is shown in Fig. 3 to highlight peak broadening differences. XRD powder patterns for all samples were compared to dolomite or calcite standard patterns.

Diffraction Peak Profile Analysis

XRD peak broadening due to shock deformation was analyzed using both single peak profiling and Rietveld refinement of peak shape parameters, both of which were carried out using Jade 8.0 software (Materials Data Corporation). With single peak profiling, the peak full width half maximum (FWHM) values are not appreciably affected by small variations in sample composition, therefore they are potentially useful for distinguishing weakly from more intensely shocked samples (Fig. 4). Peak broadening can also be analyzed by Rietveld crystal structure refinement (Young 1993) of the peak shape parameters (Skála and Jakeš 1999). XRD peak FWHM values are a function of the diffraction angle theta and three least squares refineable parameters U, V, and W (Caglioti 1958).

$$(\mathrm{FWHM})^2 = \mathrm{UTan}^2\ \mathrm{theta} + \mathrm{Vtan\ theta} + \mathrm{W}$$

The values of FWHM, which are related to the amount of shock-induced deformation, were calculated over the range 15°–120° 2θ. Single peak and Rietveld refined FWHMs were then fitted with a fourth order polynomial (Fig. 5).

RESULTS

Diffraction Patterns: Limestone

XRD patterns of calcite-rich Mission Canyon Formation samples are compared with calcite-rich Sierra Madera samples (Fig. 3a). Samples obtained from the central uplift of Sierra Madera display more peak broadening than those from the crater rim with an almost complete disappearance of peaks at 58° and 63° in sample Kwf 4. Although XRD peaks of Mission Canyon Formation sample SH 1 (Fig. 3a) are broader than crater rim samples from Sierra Madera (Kwf 1, Kwf 2, and Kwf 3), in general, calcite-rich Sierra Madera samples show more peak broadening than calcite-rich Mission Canyon Formation samples. Some Sierra Madera and Mission Canyon samples contain extra peaks. Samples Kwf 2, Kwf 4, Kwf 5 and SM 1 contain minor quartz peaks while samples SH 1 and CB 1 contain minor anhydrite peaks (Fig. 3).

Diffraction Patterns: Dolomite

Of the 14 unshocked samples collected from the Austin Core Facility only two, one from the Queen Formation and one from the Yates Formation, are dolomite. The remaining 12 samples contained dolomite with significant amounts of quartz and anhydrite and are therefore not compared to the shocked samples from Sierra Madera. XRD patterns of dolomite-rich Sierra Madera samples are compared with two unshocked equivalent samples of the Queen and Yates Formations (Fig. 3.3B). Shocked samples from Sierra Madera have more peak broadening than the unshocked Queen and Yates samples. For example, note broadening between sample Yates/Gil and Pw in the 60° and 67.5° regions.

Samples from Sierra Madera show an increase in peak broadening towards the central uplift of the impact structure. For some samples (Pw, Ph, and Pv) peak broadening is great enough to result in almost a complete disappearance of the three peaks in the 64° to 66° 2θ range.

For Mission Canyon Formation samples, patterns of samples from locations close to the Antler Orogenic front have less peak broadening than those from farther away. For example, the peaks for sample UP 1 (location 4; Fig. 3.2A) are sharper than those for sample SM 2 (location 2); especially note the three peaks in the 64° to 66° region. In general, dolomitic Sierra Madera samples have considerably more peak broadening than Mission Canyon Formation and unshocked Queen and Yates samples.

Single Peak Profiling—Full Width Half Maximum (FWHM)

The FWHM curves (Fig. 4a, b) that deviate most from the standard curves (CALSTD and DOLSTD) are those that experienced higher shock (shatter cones, monomict impact breccias and samples from the crater rim). Unshocked Queen and Yates samples plot close to the standard curve. Also the majority of the Mission Canyon Formation samples tend to plot between the scans of the standards and those of the Sierra Madera samples (with the exception of BM 2 and SH 1; Figs. 4a, 4b). However, some samples (CB 1 and Mlb 1, for example) have a convex curve instead of the expected concave curve as seen in the calcite and dolomite standards.

Rietveld Refinement of Peak Shape Parameters

FWHM curves (Fig. 5a) for calcite-rich Mission Canyon Formation samples SH 1 and BM 1 overlap calcite-rich Sierra Madera crater rim samples Kwf 3 and Kwf 1/Kwf 2, respectively. FWHM values obtained from Rietveld crystal structure refinements increase with shock intensity for all calcite-rich Sierra Madera samples. FWHM values of shocked dolomite from the central uplift of Sierra Madera are distinctly higher than dolomite from unshocked Queen and Yates samples as well as samples from the tectonically deformed dolomite from the Mission Canyon Formation (Fig. 5b) and follow a pattern of progressive broadening from crater rim to central uplift. Sierra Madera samples with shock features (shatter cones, monomict breccia) have

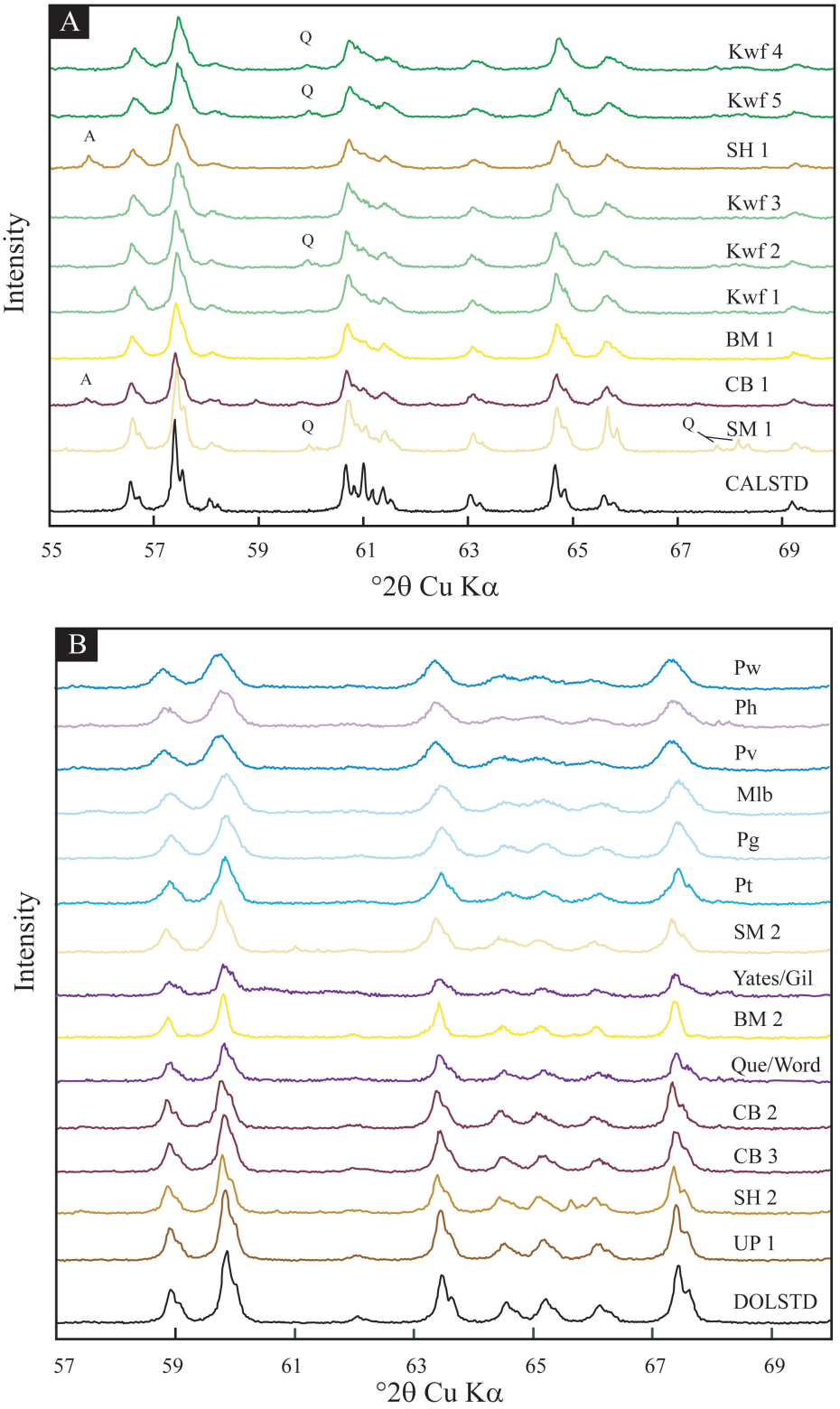

Fig. 3. X-ray powder diffraction patterns of calcite and dolomite samples from the Sierra Madera impact structure, unshocked equivalent rocks, and Lower Mississippian Mission Canyon Formation. a) Calcite-rich samples compared with the calcite standard (CALSTD). b) Dolomite-rich samples compared with the dolomite standard (DOLSTD). All scans were arranged from least (bottom of chart) to most (top of chart) broadened. See Table 1 for sample descriptions.

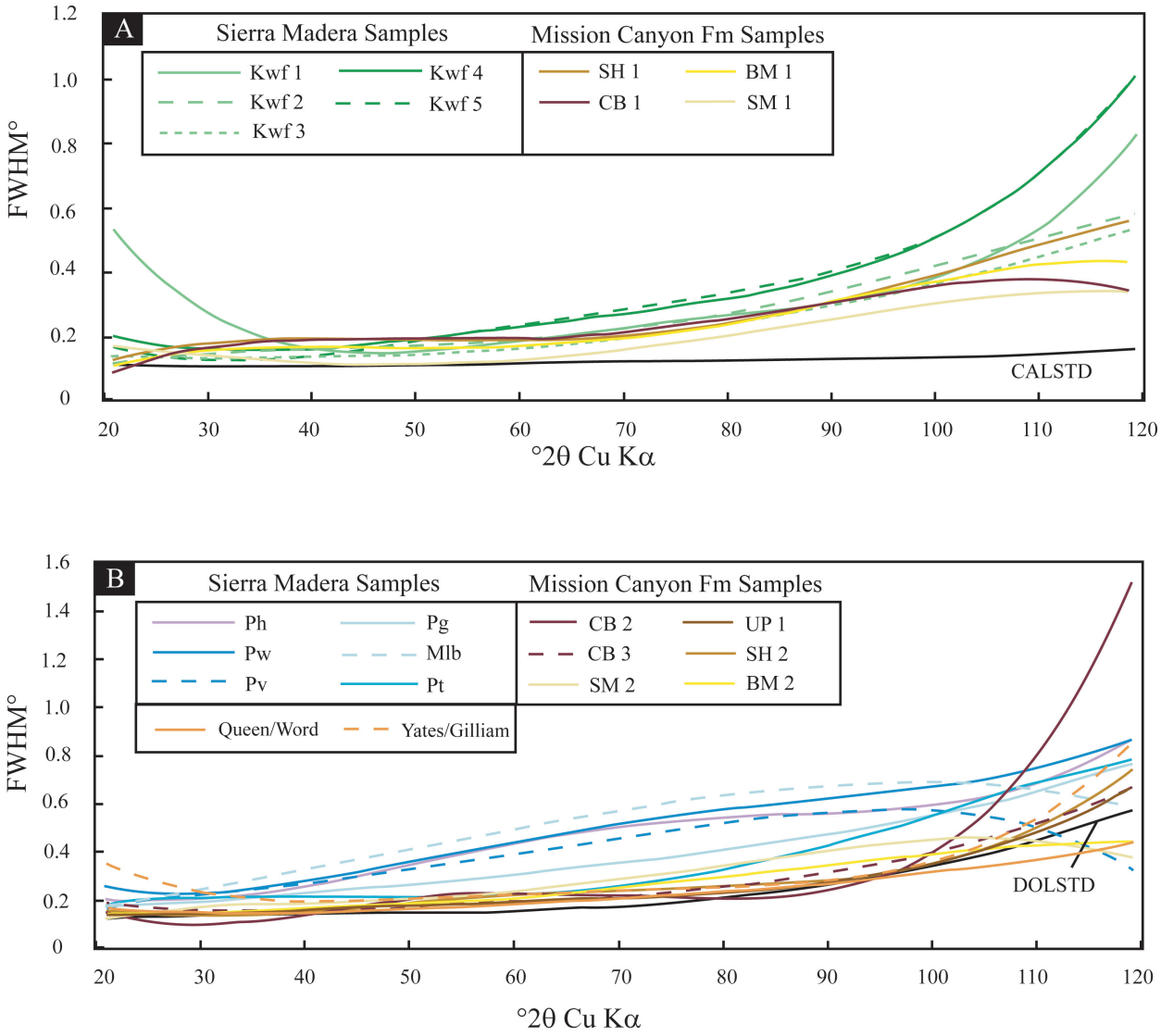

Fig. 4. Single peak profiling using FWHM values for Sierra Madera, unshocked equivalent samples, and Mission Canyon Formation samples. a) Calcite values compared with a calcite standard, CALSTD. b) Dolomite values compared with a dolomite standard, DOLSTD.

uniformly higher FWHM values than those without shock features.

DISCUSSION

All XRD peak patterns deviate from those of the calcite and dolomite standards. This is particularly true for calcite and dolomite from the central uplift of Sierra Madera. Several factors contribute to XRD peak profile variability including Mg content (Gavish and Friedman 1973), grinding time of powder (Burns and Bredig 1956; Gavish and Friedman 1973), grain size of powder (Klug and Alexander 1974; Langford et al. 2000), and phase transformations (Burns and Bredig 1956; Merrill and Bassett 1975; Fiquet et al. 1994). The above mentioned factors were considered when preparing samples for this study. The Mg, Fe, and Ca contents of all carbonate samples were measured (Table 2) and while all samples deviate slightly from the calcite and dolomite stoichiometric values, there is no correlation between composition and variability in XRD peak profiles or Rietveld refined FWHM curves. The grain size of the powder used was <27 μm as a larger crystallite size can lead to inaccurate and imprecise intensity measurements (Bish and Reynolds 1989). Phase transformations (e.g., calcite to aragonite due to grinding; Burns and Bredig 1956) were not a factor as XRD powder patterns for samples from Sierra Madera show no peaks other than those of dolomite, calcite, and in a few cases, quartz and anhydrite (Fig. 3). Quartz is a common mineral in nearshore carbonate rocks. The Mission Canyon Formation contains anhydrite and other evaporitic minerals due to evaporitic tidal flat depositional environments (Dorobek et al. 1993).

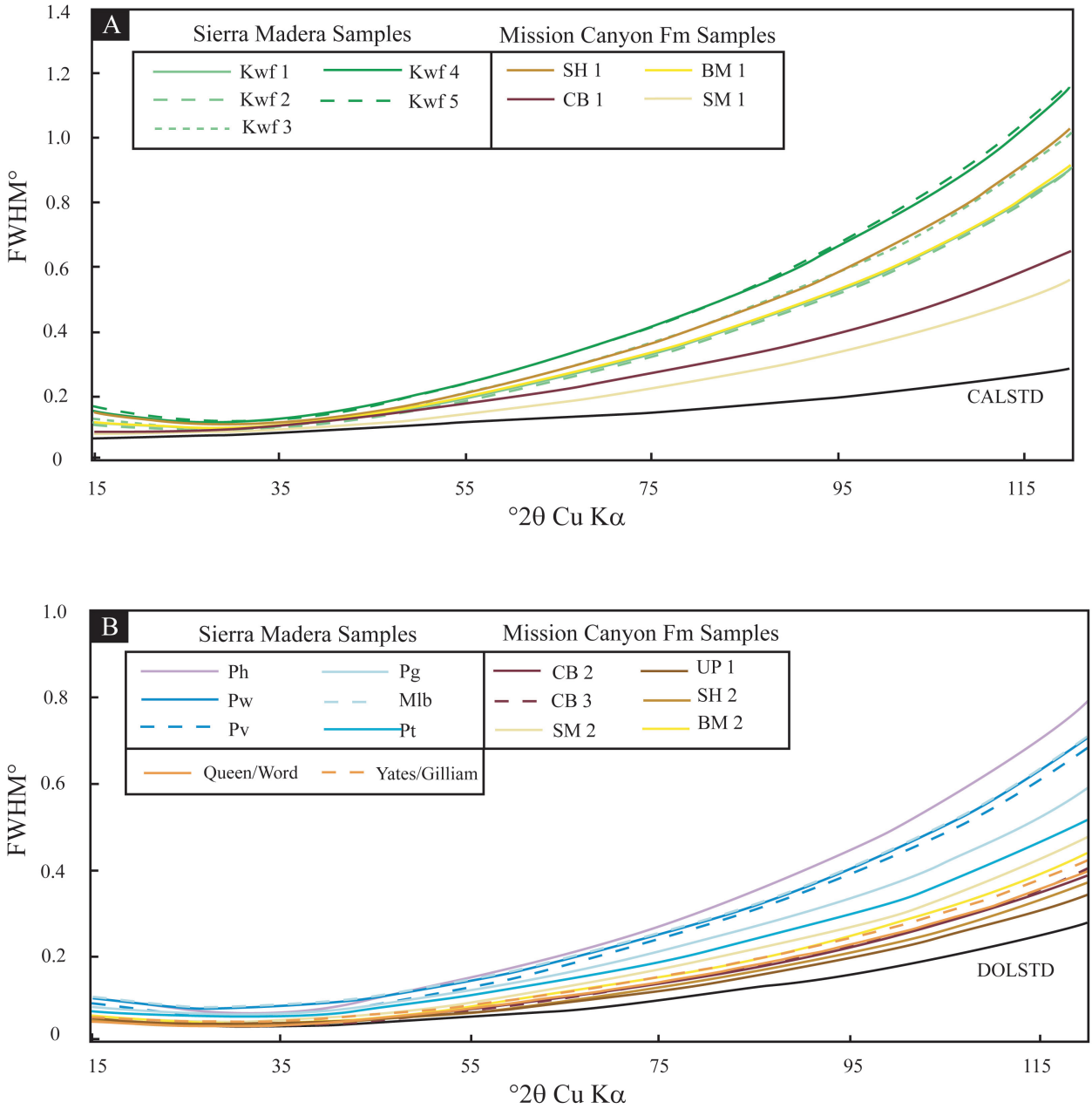

Fig. 5. Rietveld refinement analysis for Sierra Madera, unshocked equivalent samples, and Mission Canyon Formation samples. a) Calcite values compared with a calcite standard, CALSTD. b) Dolomite values compared with a dolomite standard, DOLSTD.

Single peak profile patterns of calcite and dolomite from all samples while useful at lower 2θ values, are complex and indicate little relationship to shock intensity at higher 2θ values. This is because weaker high angle reflections are poorly estimated by the profile shape function. High angle reflections from shocked material may disappear from the pattern since these reflections are often low intensity and shocking decreases the degree of the crystallinity (Skála and Jakeš 1999). While single peak profiling may be useful at lower 2θ values, at higher values, especially above ~80° 2θ, the method is unreliable.

More useful for this study was the Rietveld refinement of peak shape parameters. Rietveld refinement of peak shape parameters yields better resolution of overlapping diffraction peaks and a more precise measure of the 2θ angular dependence of peak FWHM, thus, providing a better measure of the degree of shock deformation (Skála and Jakeš 1999).

Rietveld results for the mildly shocked calcite samples from the crater rim overlap with those of Mission Canyon Formation calcite samples, whereas those of the central uplift are distinguishable from Mission Canyon Formation samples.

Dolomite samples from Sierra Madera also show increasing Rietveld refined FWHM values as the central uplift is approached reflecting increasing deformation of the dolomite crystal structure with increasing shock pressure (Skála and Jakeš 1999). Noticeably, Sierra Madera samples plot well above unshocked equivalent dolomite-rich samples from outside the crater. Therefore, XRD with Rietveld refinement analysis indicates that it may not always be possible to distinguish calcite-rich samples subjected to terrestrial tectonic processes from those mildly shocked in an impact event. However, with exposure to increasing shock pressures within the central uplift of the structure, dolomitic impact shocked rocks are readily distinguished from dolomitic unshocked rocks from outside of the structure and other terrestrially deformed dolomitic rocks.

Interestingly, Mission Canyon Formation samples do not indicate a systematic variation in Rietveld-refined FWHMs with distance from the Sevier and Laramide orogenic fronts. With Mission Canyon Formation samples, due to deformation associated with increasing compression and burial depth, peak broadening was expected to increase as sample locations approach the tectonic front of the Sevier and Laramide Orogenies (Fig. 2). The ideal and expected order for sample locations, from least to most peak broadening, is Sheep Mountain (SM), Benbow Mine (BM), Shoshone Canyon (SH) to Church Buttes (CB). However, observed XRD patterns for Mission Canyon Formation samples indicate that peak breadth increases in the order SM 1 to CB 1 to BM 1 to SH 1. The fronts of these orogens may be more complicated, with deformation unequally distributed along thrust fronts or out of phase thrusting may have occurred. Similarly, tectonic forebulge versus foreland basin events overprinted burial deformation of the Antler orogeny, increasing the complexity of the deformational history in the area. Additionally, secondary alteration of the Mission Canyon Formation associated with burial and recrystallization (Smith and Dorobek 1993) may also have affected XRD parameters; however, precipitation of secondary dolomite, one potential cause of the unexpected order, can be ruled out as it should result in peak profiles more similar to those of the standard.

Hydrothermal and Secondary Alteration in Sierra Madera

Hydrothermal and secondary alteration in rocks may affect XRD peak patterns due to modification of the original rock material. Evidence of fluorite crystals occurring in some polymict breccia outcrops (Wilshire et al. 1972) indicate hydrothermal alteration occurred as a post-impact process at Sierra Madera. However, it is not uncommon for impact craters to interact with the hydrosphere either as a disruption of the local water table or on a larger scale such as an ocean basin (Osinski et al. 2001). Rocks at Sierra Madera were not deformed after the impact event (Wilshire et al. 1972). Therefore, if hydrothermal alteration occurred at Sierra Madera, it was directly related to the impact event and not due to a subsequent deformational process.

Interestingly, XRD samples from smaller impact structures that do not develop post-impact hydrothermal systems, like Meteor Crater, show broadening. In the case of Meteor Crater, XRD samples show peak broadening but not in the expected pattern, i.e., decrease in broadening from crater center to crater rim. The results have been attributed to a pre-impact structural joint pattern in the target rocks (Burt and Pope 2001; Burt et al. 2005). Hydrothermal alteration may be a factor in XRD peak broadening patterns, however, it is not the cause of peak broadening in individual samples.

Shock Pressures and XRD Broadening

Using the shock classification scheme for impact metamorphosed sandstones developed by Kieffer (1971) and modified by Osinski (2007), we can assign shock pressure values to $CaCO_3$ cemented sandstones at Sierra Madera and apply those values to the adjacent carbonate units. Impact metamorphosed sandstones at Sierra Madera give a shock pressure range from 5.5–20 GPa based on the presence of "toasted" quartz, a "jigsaw" interlocking texture between quartz grains, and multiple sets of planar deformation features (PDFs) within quartz grains. The presence of well-developed shatter cones in porous sandstone indicates a shock pressure range of 3–10 GPa and corresponds to a post-shock temperature range of 350–>1000° C (Osinski 2007).

Sandstone beds within the Gilliam Limestone have the greatest amount of deformational features and, therefore, one would assume XRD peak patterns from the adjacent limestone would be the broadest of all Sierra Madera samples. However, the broadest XRD peak patterns come from the Hess Formation located within the center of the central uplift (Fig. 3). While the adjacent quartz-rich Cathedral Mountain Formation and sandstone beds within the Word Formation contain shock features (multiple sets of PDFs and the generation of quartz microbreccia), these units are matrix-supported, not grain-supported like the sandstone beds within the Gilliam Limestone. Without the interaction between quartz grains, higher shock pressure indicators are not present within the Cathedral Mountain Formation and Word Formation. Therefore, shock features within these two quartz-rich units do not accurately indicate the highest shock pressures to which these rocks or the adjacent limestones were exposed. Nevertheless, the presence of shatter cones within the Hess, Cathedral Mountain, and Word Formations indicate rocks from the central uplift of Sierra Madera were exposed to shock pressures in the range of 3–10 GPa; however the actual pressure range of formation is probably narrower (French 1998; Baratoux and Melosh 2003; Wieland et al. 2006; Osinski 2007).

CONCLUSIONS

Rietveld refined parameters (especially XRD peak FWHM) potentially can be used to distinguish impact-shocked rocks from unshocked equivalent rocks from outside the structure. However, this study suggests that when comparing shocked rocks to those exposed to mild tectonic deformation, shock pressures must reach at least 3–10 GPa to make this distinction, as only samples from the central uplift of Sierra Madera have significantly higher FWHM values (peak broadening) than the tectonically deformed Mission Canyon Formation samples. Similarly, it is not known how a sample exposed to intense tectonic deformation compares to a shocked sample. The Mission Canyon Formation was never exposed to intense forces associated with direct convergent boundary contact. Instead the formation was only associated with the distal edge of two orogenies, the Sevier and Laramide. If the XRD patterns of less intensely deformed Mission Canyon Formation calcites and dolomites are indistinguishable from those exposed to lower shock levels along the crater rim of Sierra Madera, it is conceivable that minerals severely deformed by tectonic processes will also be indistinguishable from higher shocked rocks from the central uplift of an impact structure. Therefore, a study of more highly shocked rocks from a different impact structure and similar rock types from a more intense tectonic setting should be carried out to further determine the usefulness of Rietveld analysis and X-ray diffraction as a tool for the characterization of impact deformed rocks.

Acknowledgments—The authors would like to thank David Katz of the University of Miami for providing Mission Canyon Formation samples and James Donnelly at the Austin Core Facility in Austin, Texas for allowing SAH access to collect unshocked carbonate samples from cores located north of Sierra Madera. Additional thanks goes to Glenn Lang and the Lyda Family who provided access to the Sierra Madera impact structure. This manuscript benefited from constructive reviews by E. Buchner, R. Skála, P. Buchanan and W. U. Reimold. This work was supported by NASA Grant NNX06AE69G and funding provided by the Barringer Crater Company.

Editorial Handling—Dr. W. U. Reimold

REFERENCES

Baratoux D. and Melosh H. J. 2003. The formation of shatter cones by shock wave interference during impacting. *Earth and Planetary Science Letters* 216:43–54.

Bish D. L. and Reynolds R. C. 1989. Sample preparation for X-ray diffraction. In *Modern powder diffraction*, edited by Bish D. L. and Post J. E. Washington D. C.: Mineralogical Society of America. pp. 73–99.

Burns J. H. and Bredig M. A. 1956. Transformation of calcite to aragonite by grinding. *Journal of Chemical Physics* 25:1281.

Burt J. B. and Pope M. C. 2001. Shock-induced effects of calcite crystals within the Kaibab Limestone at Meteor Crater, Arizona (abstract). *Geological Society of America Abstracts with Programs* 33:383.

Burt J. B., Pope M. C., and Watkinson A. J. 2005. Petrographic, X-ray diffraction, and electron spin resonance analysis of deformed calcite: Meteor Crater, Arizona. *Meteoritics & Planetary Science* 40:296–305.

Caglioti G., Paoletti A., and Ricci F. P. 1958. Choice of collimators for a crystal spectrometer for neutron diffraction. *Nuclear Instruments and Methods* 3:223–228.

Dietz R. S. 1960. Meteorite impact suggested by shatter cones in rock. *Science* 131:1781–1784.

Dorobek S. L., Smith T. M., and Whitsitt P. M. 1993. Microfabrics and geochemistry of meteoritically altered dolomite in Devonian and Mississippian carbonates, Montana and Idaho. In *Carbonate microfabrics*, edited by Rezak R. and Lavoie D. L. New York: Springer-Verlag. pp. 205–225.

Earth Impact Database. http://www.unb.ca/passc/ImpactDatabase. Accessed June 15, 2008.

Eggleton R. E. and Shoemaker E. M. 1961. Breccia at Sierra Madera. USGS Professional Paper 424-D. pp. D151–D153.

Fiquet G., Guyot F., and Itié J. 1994. High-pressure X-ray diffraction study of carbonates: $MgCO_3$, $CaMg(CO_3)_2$, and $CaCO_3$. *American Mineralogist* 79:15–23.

Foit F. F. Jr. 1992. X-ray and optical data for a vanadium-rich dravite from Silver Knob, Mariposa County, California, USA. *Powder Diffraction* 7:236–238.

French B. M. 1998. *Traces of catastrophe: A handbook of shock-metamorphic effects in terrestrial meteorite impact structures*. Houston: Lunar and Planetary Institute. 120 p.

Gavish E. and Friedman G. M. 1973. Quantitative analysis of calcite and Mg-calcite by X-ray diffraction: Effect of grinding on peak height and peak area. *Sedimentology* 20:437–444.

Grieve R. A. F. 1998. Extraterrestrial impact on Earth: The evidence and the consequences. In *Meteorites; flux with time and impact effects*, edited by Grady M. M., Hutchison R., McCall G. J. H., and Rothery D. A. London: Geological Society of London Special Publication 140. pp. 105–131.

Grieve R. A. F., Langenhorst F., and Stöffler D. 1996. Shock metamorphism of quartz and experiment: II. Significance in geoscience. *Meteoritics & Planetary Science* 31:6–35.

Grieve R. A. F. and Robertson P. B. 1979. The terrestrial cratering record. 1, Current status of observations. *Icarus* 38:212–229.

Hill C. A. 1996. Geology of the Delaware Basin, Guadalupe, Apache, and Glass Mountains, New Mexico and West Texas: SEMP, Permian Basin Section, Publ. 96–39. 480 p.

Hörz F. 1968. Statistical measurements of deformation structures and refractive indices in experimentally shock loaded quartz. In *Shock metamorphism of natural materials*, edited by French B. M. and Short N. M. Baltimore: Mono Book Corp. pp. 243–253.

Hörz F. and Quaide W. L. 1973. Debye-Scherrer investigations of experimentally shocked studies. *The Moon* 6:45–82.

Howard K. A. and Offield T. W. 1968. Shatter cones at Sierra Madera, Texas. *Science* 162:261–265.

Howard K. A., Offield T. W., and Wilshire H. G. 1972. Structure of Sierra Madera, Texas, as a guide to central peaks of lunar craters. *Geological Society of America Bulletin* 83:2795–2808.

Huson S. A., Pope M. C., Watkinson A. J., and Foit F. F. Jr. 2005. Possible planar elements in zircon as an indicator of peak impact pressures from the Sierra Madera impact crater, West Texas (abstract #2048). 36th Lunar and Planetary Science Conference. CD-ROM.

Huson S. A., Foit F. F. Jr., and Pope M. C. 2006a. X-ray diffraction study at Sierra Madera impact structure, West Texas (abstract). *Geological Society of America Abstracts with Programs* 38:81.

Huson S. A., Foit F. F. Jr., Watkinson A. J., and Pope M. C. 2006b. X-ray diffraction powder patterns and thin section observations from the Sierra Madera impact structure (abstract #2377). 37th Lunar and Planetary Science Conference. CD-ROM.

Kieffer S. W. 1971. Shock metamorphism of the Coconino Sandstone at Meteor Crater, Arizona. *Journal of Geophysical Research* 76: 5449–5473.

Klug H. P. and Alexander L. E. 1974. *X-ray diffraction procedures*, 2nd ed., New York: John Wiley and Sons. 966 p.

Langford J. I., Louër D., and Scardi P. 2000. Effect of a crystallite size distribution of X-ray diffraction line profiles and whole-powder-pattern fitting. *Journal of Applied Crystallography* 33: 964–974.

Merrill L. and Basset W. A. 1975. The crystal structure of $CaCO_3$(II), a high-pressure metastable phase of calcium carbonate. *Acta Crystallographica* B31:343–349.

Osinski G. R. 2007. Impact metamorphism of $CaCO_3$-bearing sandstones at the Haughton structure, Canada. *Meteoritics & Planetary Science* 42:1945–1960.

Osinski G. R., Spray J. G., and Lee P. 2001. Impact-induced hydrothermal activity within the Haughton impact structure, arctic Canada: Generation of a transient, warm, wet oasis. *Meteoritics & Planetary Science* 36:731–745.

Reimold W. U. 2007. The impact crater bandwagon (some problems with the terrestrial impact cratering record). *Meteoritics & Planetary Science* 42:1467–1472.

Ryder G. 2002. Mass flux in the ancient Earth-Moon system and benign implications for the origin of life on Earth. *Journal of Geophysical Research* 107:6-1–6-13.

Sando W. J. 1976. Mississippian history of the Northern Rocky Mountains Region. *Journal of Research United States Geologic Survey* 4:317–338.

Sando W. J. 1988. Madison Limestone (Mississippian) paleokarst: A geologic synthesis. In *Paleokarst* edited by James N. P. and Choquette P. W. New York: Springer-Verlag. pp. 256–277.

Short N. M. 1968. Nuclear-explosion-induced microdeformation in rocks: An aid to recognition of meteorite impact structures. In *Shock metamorphism of natural materials*, edited by French B. M. and Short N. M. Baltimore: Mono Book Corp. pp. 185–210.

Skála R. and Jakeš P. 1999. Shock-induced effects in natural calcite-rich targets revealed by X-ray powder diffraction. Geological Society of America Special Paper 339. pp. 205–214.

Smith T. M. and Dorobek S. L. 1993. Alteration of early-formed dolomite during shallow to deep burial: Mississippian Mission Canyon Formation, central to southwestern Montana. *Geological Society of America Bulletin* 105:1389–1399.

Snoke A. W. 1993. Geologic history of Wyoming within the tectonic framework of the North American Cordillera. *Memoir-Geologic Survey of Wyoming* 5:2–56.

Stewart S. A. and Allen P. J. 2002. A 20-km-diameter multi-ringed impact structure in the North Sea. *Nature* 418:520–523.

Underhill J. R. 2004. Earth science: An alternative origin for the "Silverpit crater." *Nature* 428:280.

Wieland F., Reimold W. U., and Gibson R. L. 2006. New observations on shatter cones in the Vredefort impact structure, South Africa, and evaluation of current hypotheses for shatter cone formation. *Meteoritics & Planetary Science* 41:1737–1759.

Wilshire H. G. and Howard K. A. 1968. Structural pattern in central uplifts of cryptoexplosion structures as typified by Sierra Madera. *Science* 162:258–261.

Wilshire H. G., Offield T. W., Howard K. A., and Cummings D. 1972. Geology of the Sierra Madera Cryptoexplosion Structure, Pecos County, Texas. USGS Professional Paper 599-H. pp. 1–49.

Young R. A. 1993. *The Rietveld method*. Oxford: Oxford University Press. 298 p.